J. Exp. Biomed. Sci. 11 (2005) 31-36

Vasogenic Edema in Experimental Cerebral Fat Embolism

Byung-Rae Park[1†] and Bong-Oh Koo[2]

[1]Department of Radiological Science, [2]Department of Physical Theraphy, Catholic University of Pusan, Busan 609-757, Korea

To evaluate the magnetic resonance imaging and electron microscopic findings of the hyperacute stage of cerebral fat embolism in cats and the time needed for the development of vasogenic edema. Magnetic resonance imaging was performed at 30 minutes (group 1, n=9) and at 30 minutes and 1, 2, 4, and 6 hours after embolization with triolein (group 2, n=10). As a control for group 2, the same acquisition was obtained after embolization with polyvinyl alcohol particles (group 3, n=5). Electron microscopic examination was done in all cats. In group 1, the lesions were iso- or slightly hyperintense on T2-weighted (T2W) and diffusion-weighted (DWIs) images, hypointense on the apparent diffusion coefficient (ADC) map image, and markedly enhanced on the gadolinium-enhanced Tl-weighted images (Gd-T1WIs). In group 2 at 30 minutes, the lesions were similar to those in group 1. Thereafter, the lesions became more hyperintense on T2WIs and DWIs and more hypoinfense on the ADC map image. In group 3, the lesions showed mild hyperintensity on T2WIs at 6 hours but hypointensity on the ADC map image from 30 minutes, with a tendency toward a greater decrease over time. Electron microscopic findings revealed discontinuity of the capillary endothelial wall, perivascular and interstitial edema, and swelling of glial and neuronal cells in groups 1 and 2. The lesions were hyperintense on T2WIs and DWIs, hypointense on the ADC map image, and enhanced on Gd-T1WIs. On electron microscopy, the lesions showed cytotoxic and vasogenic edema with disruption of the blood-brain barrier.

Key Words: Fat embolism, Vasogenic edema, Brain, Magnetic resonance imaging (MRI)

INTRODUCTION

Fat embolism is associated primarily with osseous fractures of long bones (Drew et al., 1995) and the clinical fat embolism syndrome has been reported in up toll 11% of cases (Fabian et al., 1990). Neurological signs have been reported in up to 100% of patients with the fat embolism syndrome (Bouaggad et al., 1995) including paresis or paralysis, convulsions, delirium, confusion, and stupor, which may progress to coma (Weisz et al., 1971) Magnetic resonance imaging (MRI) studies using T2-weighted (T2WI) and diffusion-weighted (DWI) images are well-established tools for the evaluation of acute ischemic infarction. Diffusion-weighted imaging studies offer a new approach for imaging abnormalities rapidly after the onset of ischemia (Moseley et al., 1990). The high signal intensities seen on DWIs and the differences in the diffusion coefficient of biological water in different environments suggest cytotoxic edema (Moseley et al., 1990). However, T2WIs are less useful in the diagnosis of hyperacute ischemia because they require several hours from the onset of stroke before demonstrating abnormalities. Furthermore, gadolinium-enhanced Tl-weighted images (Gd-TlWIs) show no lesional enhancement in hyperacute infarction. A study of cerebral arterial fat embolism in rats with the use of radioisotopes (Drew et al., 1998) has shown that the blood-brain barrier is damaged and opened within the first 15 minutes due to the fat embolus. Our hypothesis is that if cerebral · fat embolism causes an early breakdown of the blood-brain barrier, then MRI findings would differ from those described in ischemic infarction. However, there have been no experimental or clinical reports studying the hyperacute stage of cerebral fat embolism by MRI. The triglyceride triolein is the predominant fat in bone marrow and is reported to be the major constituent of embolized fat in humans (Jones et al., 1982). It has a freezing point of 40℃, and thus, it remains

*Received: January 11, 2005
Accepted after revision: February 12, 2005
†Corresponding author: Byung-Rae Park, Department of Radiological Science, Catholic University of Pusan, #9, Bugok 3-dong, Geumjeong-gu, Busan 609-757, Korea
Tel: 051-510-0583, Fax: 051-510-0588, e-mail: brpark@cup.ac.kr

liquid at body temperature and is immiscible with plasma. This study was performed to evaluate the findings on MRI, including T2WI, DWI, the apparent diffusion coefficient (ADC) map image, and Gd-TlWI and to correlate them with electron microscopic findings with the aim of evaluating the changes in the blood-brain barrier in a cat model of cerebral fat embolism.

MATERIALS AND METHODS

1. Animal model and experimental design of Fat embolism and control groups

All experimental protocols were approved by the institutional animal review board. Cats (2.8~3.3 kg) were anesthetized with an intramuscular injection of ketamine HCl (2.5 mg/kg; Korea United Pharm Inc., Seoul, Korea) and xylazine (0.125 mg/kg; Bayer Korea, Seoul, Korea). Body temperature was measured with a rectal probe (MGA-III 219, Shibaura Electronics Co. Ltd., Tokyo, Japan) and maintained at 37℃ to 37.5℃. Respiration rate was checked before, during, and after the procedure. Catheters were placed in the left femoral artery to allow monitoring of blood pressure and blood gas levels and in the left femoral vein for injection of contrast material. The right femoral artery was isolated and the distal portion ligated with 4.0 silk. An 18-gauge intravenous catheter (Insyte, Becton Dickinson, Sandy, UT) was inserted into the artery. A 3.0F microcatheter (MicroFerret-18 infusion catheter, William Cook Europe, Bjaeverskov, Denmark) was passed through the intravenous catheter into the lumen of the artery, and either the right or the left internal carotid artery was selected. The tip of the microcatheter was positioned just proximal to the origin of the carotid plexus to limit extracranial accumulation of fat.

The cats were divided into three groups: group 1 (n=9, 30-minute acquisition only) and group 2 (n=10, 30-minute and 1-, 2-, 4-, and 6-hour acquisitions) were given a single dose of 0.1 ml of the neutral triglyceride triolein (1,2,3tri [cis-9-octadecenoyl]-glycerol, 99% purity, d=0.91 g/ml; Sigma, St. Louis, MO) followed by 2 ml saline over a period of 30 seconds; group 3 (n=5) was given 10 mg of 45- to 150-μm polyvinyl alcohol immersed in 10 ml saline instead of the triolein as a nonfat control group. The triolein, which was stored, sealed, and frozen between use to minimize chemical denaturation, was warmed to body temperature just before injection.

2. Magnetic resonance imaging

Magnetic resonance scanning commenced 30 minutes after embolization. The cats were placed in a prone position within a pediatric MR infant restrainer, and a small FOV coil (Siemens, Erlangen, Germany) was placed above the head. All studies were performed on a 1.5-T MR Vision scanner using standard hardware. For T2W sequences, scan parameters were as follows: repetition time = 3000 ms, echo time = 96 ms, section thickness = 4 mm with a 0.1-mm gap field of view = 70 to 75 mm, two excitations, acquisition matrix = 210×256. Diffusion-weighted imaging was performed using an echo planar sequence. The imaging parameters were as follows: field of view = 130 mm, phase-encoding steps = 128, section thickness = 4 mm with a 0.1-mm gap, acquisition matrix = 96×160. The diffusion-sensitizing gradient was oriented along the y axis (ventral to dorsal) with *b* values of 0 and 1000 seconds/mm^2. The ADC mapping was done with custom software on a pixel-by-pixel basis with the aid ofthe following equation: ADC = In $(S_0/S_1) / (b_1-b_0)$, where S_0 and S_1 are the signals of the two DWIs. Gadolinium-enhanced T1 WIs were acquired with 0.2 mmol/kg gadopentetate dimeglumine (Magnevist, Schering, Germany) with the parameters as follows: repetition time = 320 ms, echo time = 20 ms, section thickness = 4 mm with a 0.1-mm gap, field of view = 70 to 75 mm, two excitations, acquisition matrix = 210×256. In group 1, T2WIs, DWIs, the ADC map image, and GdT1 WIs were obtained 30 minutes after embolization, after which the animals were humanely killed. In groups 2 and 3, T2WIs, DWIs, the ADC map image, and Gd-Tl WIs were obtained serially at 30 minutes and 1, 2, 4, and 6 hours after embolization, after which the animals were humanely killed. All images were acquired in the coronal plane.

3. MRI analysis

1) Signal intensity

All MRIs acquired for all three groups were analyzed with respect to the presence or absence of abnormal signal intensity and the size of any abnormalities. Also, the temporal change in signal intensity was evaluated in groups 2 and 3.

2) Quantitative assessment

For quantitative assessment, signal intensity ratios (SIRs)

on T1WIs, the ADC map image, and Gd-T1WIs were measured in groups 2 and 3. The SIR was defined as the intensity ratio of a region of interest (ROI) of an obviously abnormal cortical lesion to that of the normal contralateral cortex. Signal abnormality at 6 hours after embolization was used to determine the ROI location used for all sequences at all acquisition times, including the high signal intensity seen on T1WIs, the low signal intensity on the ADC map image, and enhancement on the Gd-T1WIs. The size of the circular ROI used was 0.5 to 3 mm^2. In the assessment of serial images of the same cat, the size and position of the ROI were identical. This assessment was confined to the superficial cortex owing to the uneven location of deep gray matter in the lesions. The significance of difference in SIR between groups 1 and 2 and of the change in SIR over time was estimated from an analysis of variance on repeated measurements.

4. Electron microscopic examination

Electron microscopic examination was done in all cats of groups 1, 2, and 3. Immediately after the cats were humanely killed, the brains were cut into 4-mm-thick blocks. Six areas of gray and white matter of the lesion and of the normal contralateral hemisphere were selected by correlation with lesions seen on the MRIs. These areas were cut into 1 mm cubes. Samples were infiltrated in 2.5% glutaraldehyde in phosphate-buffered saline at pH 7.2 for 2 hours at 40℃, washed in 0.1 mol/L phosphate-buffered saline, dehydrated with alcohol, fixed en bloc overnight with resin (Poly sciences, Warrington, PA), and stored for 12 hours at 37℃ followed by 48 hours at 45℃. After 1 μm thin sections were made, the samples were stained with uranyl acetate and lead citrate and examined with a transmission electron microscope (JEM 1200 EX-II; JEOL, Tokyo, Japan).

The presence of either vasogenic or cytotoxic edema and the integrity of the blood vessels were evaluated. The features considered to be characteristic of vasogenic and cytotoxic edema were those described by Fishman (Fishman, 1975). Compared with the normal hemisphere, if the extracellular space was increased, it was described as vasogenic edema. If endothelial, glial, or neuronal cells were swollen, it was described as cytotoxic edema. Integrity of the blood vessels was evaluated on the basis of whether the endothelial wall was discontinuous or separated. When all layers of the endothelial wall were cut, the wall was described as discontinuous, and when the layers were separated along the layers rather than through the cut, the wall was described as separated.

RESULTS

1. MRI findings, signal intensity, and lesion conspicuity groups 1 and 2: Fat embolization groups

In groups 1 (n=9) and 2 (n=10), the lesions were mostly located at the ipsilateral posterior and upper lateral cerebral superficial cortex. In some cats, the ipsilateral basal ganglia or contralateral superficial upper lateral cerebral superficial cortex was involved. On T2WIs at 30 minutes, the lesion was either isointense, six in group 1 and seven in group 2, or hyperintense, three in each group (Fig. 1A). In group 2, all of the lesions were hyperintense at 1 hour, signal intensities tended to increase over time, and the hyperintensity extended to the subcortical white matter.

On DWIs at 30 minutes, the lesion was either isointense, two in group 1 (Fig. lB) and three in group 2, or hyperintense, seven in each group. Thereafter, intensity showed a tendency to increase in group 2. The size of the hyperintensity also increased slightly after 30 minutes.

The ADC map image showed either subtle hypointensity three in group 1 and four in group 2, or mild hypointensity, six in each group at 30 minutes (Fig. 1C). The hypointensity became more prominent after 30 minutes and was observed in all cats at 6 hours in group 2.

On Gd-TlWIs, the lesions were remarkably enhanced at times (Fig. 1D). At 30 minutes and 1 hour, the lesion area was larger on gadolinium-enhanced images than on T2WIs or DWIs. The lesion contrast was more conspicuous on Gd-T1WIs than on T1WIs or DWIs at those times. Enhancement of the basal ganglia, brain stem, or contralateral hemisphere was seen in several cats (Fig. lD).

2. Group 3: Control group

In group 3 (n=5) on T2WIs, the lesion was isointense at 30 minutes and 1 hour in all five cats. At 2 hours, two cats showed subtle hyperintensity. At 4 hours, two cats showed mild and two cats showed subtle hyperintensity. At 6 hours, all five cats showed mild hyperintensity. On DWIs, the lesion was hyperintense from 30 minutes, and the hyperintensity showed a tendency to increase thereafter. The ADC map image showed mild hypointensity of the lesion at 30

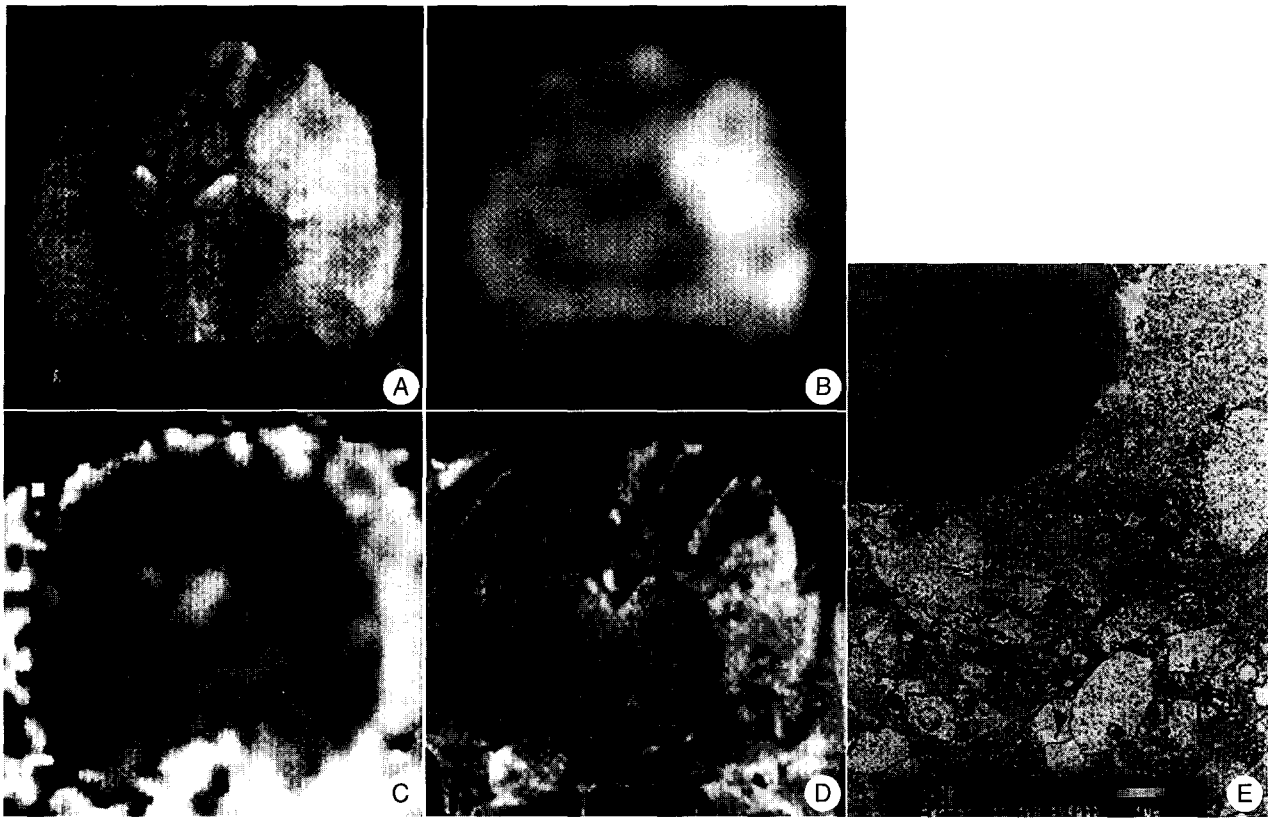

Fig. 1. Coronal magnetic resonance **(A-D)** and electron microscopic **(E)** imaging findings of a cat brain obtained 30 minutes after embolization (group 1). The lesion is hyperintense on the T2-weighted (A; repetition time [TR] = 3000 ms, echo time [TE] = 96 ms) and diffusion-weighted (B; *b* value = 1000 seconds/mm^2) images, hypointense on the apparent diffusion coefficient map image (C), and enhanced on the gadolinium-enhanced T1weighted image (0; TR/TE = 320/20) in the left superficial gray and white matter. Both basal ganglia are also slightly involved. Electron microscopic examination (E; ×5,000) of the gray matter shows intraluminal fat (*asterisk*), focal discontinuity of the capillary endothelial wall (*arrows*), microcystic change of neuropil processes (*arrowheads*), and edematous swelling of mitochondria (*open arrows*).

minutes, and the hypointensity became more and more prominent thereafter. On Gd-TlWIs, the lesion was not enhanced in four cats, although one cat showed mild leptomeningeal enhancement from 2 hours.

3. Quantitative analysis of groups 2 and 3 on MRI

The change in SIR of both groups is shown in Figs. 4 through 6. The SIRs on T2WIs were above 1.0 from 30 minutes and tended to increase thereafter. Compared with the 30-minute baseline, there was a statistically significant elevation of the SIRs thereafter (P=0.0001). Compared with the control group, the SIR of group 2 was statistically higher (P<0.05). The SIRs of both groups increased over time on the ADC map image. In group 2, the SIR decreased significantly from 2 hours compared with that at both 30 minutes and 1 hour (P=0.0002). In group 3, the SIR decreased significantly from 1 hour (P=0.0001). However, there was no statistical difference between groups 2 and 3 (P=0.6337). On the Gd-T1WIs, the SIR was statistically higher in group 2 than in group 3 at all times (P<0.05). The difference in SIR between these two groups was most prominent on the Gd-T1WIs compared with T2WIs and DWIs However, there was no significant change in the SIR over time (P=0.3359). Enhancement of the lesion in group 2 was statistically higher than that of the control group at all times (P=0.05).

4. Electron microscopic findings

1) Groups 1 and 2: Fat embolization groups

In groups 1 (n=9) and 2 (n=10), intravascular fat vacuoles and discontinuity of the endothelial walls were noticed in all cats (Fig. 1E). The size of the endothelial wall defect was about 1 to 3/μm. Many vessels were dilated with fat impacted in the vascular lumen, and the endothelial walls

were flattened. In some areas, small extraluminal fat vacuoles were noted and some of them appeared to have been phagocytized by macrophages. Extravasated red blood cells were also seen sporadically. Microcystic changes of the neuropil matrix and swollen neuronal and glial cells were prominent. These findings were predominantly seen in the gray matter. The neuronal processes and glial cells were also swollen in the white matter, and the separation of myelin sheaths was more prominent in the white matter than in the gray matter. In three cats of group 2, the neurons and glial cells were much more swollen and the separation of myelin sheaths was more prominent.

2) Group 3: Control group

There was perivascular and interstitial edema, neuronal cellular swelling, and separation of the endothelial wall in four cases. These findmgs were moderate to severe in two cases and mild in two cases. There were no discernible abnormalities in one case. The separation of the endothelial wall was infrequently seen; however, discontinuity of the endothelial wall was absent.

DISCUSSION

The major finding in this study is that vasogenic edema seems to occur earlier by way of the opened blood-brain barrier in cerebral fat embolism compared with that reported in ischemic infarction. This concept is supported by several observations. First, marked enhancement was noticeable on Gd-TlWI, suggesting disruption of the blood-brain barrier. Second, the observed high signal intensity on T2WI is, the authors believe, primarily due to vasogenic edema. Third, on electron microscopic study, disruption of the endothelial wall and interstitial edema were seen.

This study took advantage of the ability to detect alterations in blood-brain barrier permeability by Gd-TlWI. Gadolinium-enhanced images are able to show the site of blood-brain barrier breakdown (Barzo et al., 1996). In the presence of increased permeability or disruption of the blood-brain barrier, gadolinium extravasates and diffuses into the brain parenchyma. In the present study, Gd-TlWI enabled the detection of lesions due to discontinuity of the endothelial membrane as early as 30 minutes after embolization, as supported by the electron microscopic data. All of the cats in the fat embolization groups showed discontinuity of the endothelial wall, and in some areas, fat vacuoles extravasated through the discontinuous wall. Around the defect, perivascular edema was also prominent. In the control group, there was separation of the endothelial wall in three cases, and one of them showed mild enhancement starting at 2 hours. It appears important that the enhancing pattern is quite different between the fat embolization groups and the ischemic group. In most cases, the contralateral hemisphere was not enhanced on Gd-T1WI. However, several cats showed small and focal enhancement in the contralateral hemisphere, and this enhancement was believed to be due to embolization of fat through the communicating vessels and not due to the toxicity of gadolinium. This idea is supported by the fact that the cats showing enhancing contralateral lesions at 30 minutes revealed no additional

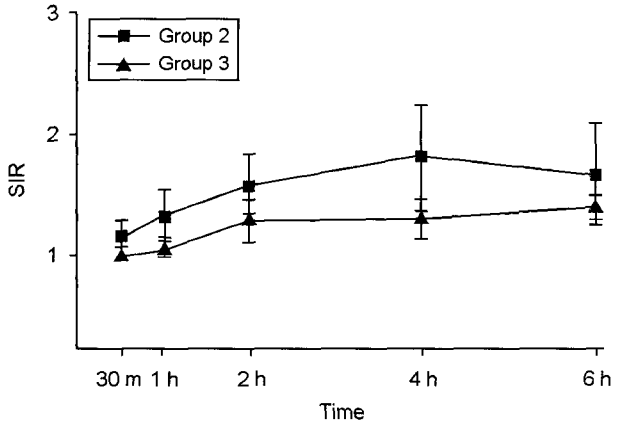

Fig. 2. Plot of signal intensity ratio (SIR) on T2-weighted images. The SIRs of both groups increased over time, and the SIR of group 2 was significantly higher than that of group 3 ($P<0.05$).

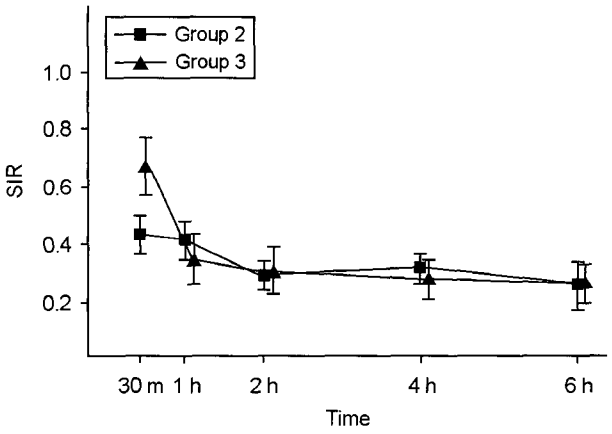

Fig. 3. Plot of signal intensity ration (SIR) on the apparent diffusion coefficient map image. In both groups, SIRs decreased over time significantly from 2 hours ($P<0.005$). However, there was no difference between groups 2 and 3 ($P=0.6337$).

enhancing areas after 30 minutes. Neurotoxicity from the repetitive gadolinium injection was not the cause of the enhancement because the enhancing areas were the same from 30 minutes to 6 hours. The hyperintensity on T2WI was progressively prominent over time from 30 minutes in group 2, while the ischemic lesions began to show mild hyperintensity from 2 hours in the control group. At 30 minutes, seven of 10 cats in group 2 showed no hyperintensity; however, the SIR was higher than 1.0 and was significantly higher than that of the ischemic control group. The SIR after 30 minutes also showed a significant difference between group 2 and group 3 (Fig. 2). The observed hyperintensity on T2WI may have been due to vasogenic edema (Pierpaoli et al., 1993). Vasogenic edema seems to be caused by free leakage of plasma fluid through the damaged capillary endothelial walls. The process of vasogenic edema is different from cytotoxic edema. Cytotoxic edema, which might be caused by depletion of high-energy phosphates, appears first and is followed by a cascade of events, resulting in vasogenic edema. T2WI taken immediately after induction of ischemia by middle cerebral arterial occlusion showed no abnormalities, and it took several hours to notice the hyperintensity (Moseley et al., 1990). In the present study, the early appearance of hyperintensity on T2WI in groups 1 and 2 compared with the ischemic control group suggests the difference in time of onset of vasogenic edema between each group. The ADC map image showed low signal intensity in groups 2 and 3. The signal intensity further decreased over time (Fig. 3). This finding suggests that cytotoxic edema also occurred early in both the fat embolization and the ischemic control groups. The swollen neuron and glial cells observed on electron microscopy provided additional evidence for the occurrence of cytotoxic edema. This result is similar to that described in the literature when ischemic models have been employed.

In this study, *b* values in DWI were 0 and 1000 seconds/mm^2. The hyperintensity on DWI with a *b* value of 1000 was nearly equal to the hypointensity on the ADC map image. Interpretation of DWIs obtained with *b* values greater than 1000 seconds/mm^2 must consider the increasing contribution of diffusion weighting and the diminished T2 effects (DeLano et al., 2000).

In conclusion, the lesions produced in this experimental model of cerebral fat embolism were hyperintense on T2WI and DWI, hypointense on the ADC map images, and enhanced on Gd-TIWI in the hyperacute stage. Electron microscopy of the lesion showed cytotoxic and vasogenic edema with disruption of the blood-brain barrier. Vasogenic edema seems to develop within 30 minutes through the disrupted blood-brain barrier in cerebral fat embolism in cats.

REFERENCES

Barzo P, Marmarou A, Fatouros P. Magnetic resonance imaging-monitored acute blood-brain barrier changes in experimental traumatic brain injury. J Neurosurg. 1996. 85: 1113-1121.

Bouaggad A, Harti A, Elmouknia M. Neurologic manifestations of fat embolism. Can Anesthesiol. 1995. 43: 441-443.

DeLano MC, Cooper TG, Siebert IE. High-*b*-value diffusionweighted MR imaging of adult brain: Image contrast and apparent diffusion coefficient map features. Am J Neuroradiol. 2000. 21: 1830-1836.

Drew PA, Helps SC, Smith E. Cerebral arterial fat embolism in the rabbit. J Neurol Sci. 1995. 134: 15-20.

Drew PA, Smith E, Thomas PD. Fat distribution and changes in the blood brain barrier in rat model of cerebral arterial fat embolism. J Neurol Sci. 1998. 156: 138-143.

Fabian TC, Hoots AV, Stanford DS. Fat embolism syndrome: Prospective evaluation in 92 fracture patients. Crit Care Med. 1990. 18: 42-46.

Fishman RA. Brain edema. N Engl J Med. 1975. 293: 706-711.

Moseley ME, Cohen Y, Mintorovitch J. Early detection of regional cerebral ischemia in cats: Comparison of diffusion and TI-weighted MRI and spectroscopy. Magn Reson Med. 1990. 14: 330-346.

Moseley ME, Kucharczyk J, Mintorovitch J. Diffusion-weighted MR imaging of acute stroke: Correlation with T2-weighted and magnetic susceptibility-enhanced MR imaging in cats. Am J Neuroradiol. 1990. 11: 423-429.

Jones JG, Minty BD, Beeley JM. Pulmonary epithelial permeability is immediately increased after embolisation with olein acid but not with neutral fat. Thorax. 1982. 37: 169-174.

Pierpaoli C, Righini A, Linfante I. Histopathologic correlates of abnormal water diffusion in cerebral ischemia: Diffusion-weighted MR imaging and light and electron microscopic study. Radiology. 1993. 189: 439-448.

Weisz GM, Steiner E. The cause of death in fat embolism. Chest. 1971. 59: 511-516.